2007 International Symposium on Nonlinear Theory and its Applications
NOLTA'07, Vancouver, Canada, September 16-19, 2007

Improvement to the Condition for Oscillation of Cross-Coupled Sinusoidal Oscillators

A. S. Elwakil* *senior member IEEE* and K. N. Salama** *member IEEE*

* Department of Electrical & Computer Engineering, University of Sharjah, P.O. Box 27272, Emirates. (email: elwakil@ieee.org)

** Electrical, Computer and Systems Engineering Dept., Rensselaer Polytechnic Institute, NY 12180, USA (email: khaled_salama@ieee.org)

Abstract— **We present a four-dimensional nonlinear model for classical cross-coupled LC oscillators. The widely accepted oscillation condition for this class of oscillators is shown to be non-optimum although oscillations are produced when it is satisfied. Further, a nonlinear graphical design technique is described.**

Keywords: Cross-coupled oscillators, sinusoidal oscillators.

I. Introduction

Characterizing the performance of sinusoidal oscillators is crucial for many electronic systems. Despite the contributions of various researchers, originating from a linear circuit theory perspective [1], some important characteristics of oscillators, such as latch-up and hysteresis jumps, can be predicted only using nonlinear analysis techniques [2]-[3]. Further, the type of nonlinearity inherent within any oscillator structure and whether its is monotone or non-monotone defines its behavior as a relaxation or sinusoidal oscillator and determines the oscillation amplitude [4].

Cross-coupled oscillators form a famous class of oscillators based on activating a passive LC tank resonator through a differential negative resistor [5]. They are widely used in commercial applications particularly when employed as VCO's [6]-[7]. Traditional linear analysis usually treats these oscillators as second-order systems, due to symmetry; from which the condition for oscillation according to the Barkhausen criterion is simply to ensure that the loop gain exceeds unity [8]. A classical cross-coupled oscillator is shown in Fig. 1(a). Many variants of this oscillator can be found in the literature, however, all of these variants essentially reduce to the model shown in Fig. 1(b). In particular, the cross-coupling technique connects two inverting amplifiers (symbolized in Fig. 1(b) as digital inverters for simplicity) in a closed-loop; in Fig. 1(a) each transistor along with its resistive load form one common-source amplifier. The linear analysis-based oscillation condition implies that the gain of each amplifier exceeds unity; i.e. $g_m r_L \geq 1$, where g_m is the small signal MOS transistor transconductance and r_L is the resistive load.

In this work, we derive a 4D nonlinear model and show that the condition $g_m r_L \geq 1$ is not optimum, although it does guarantee oscillations.

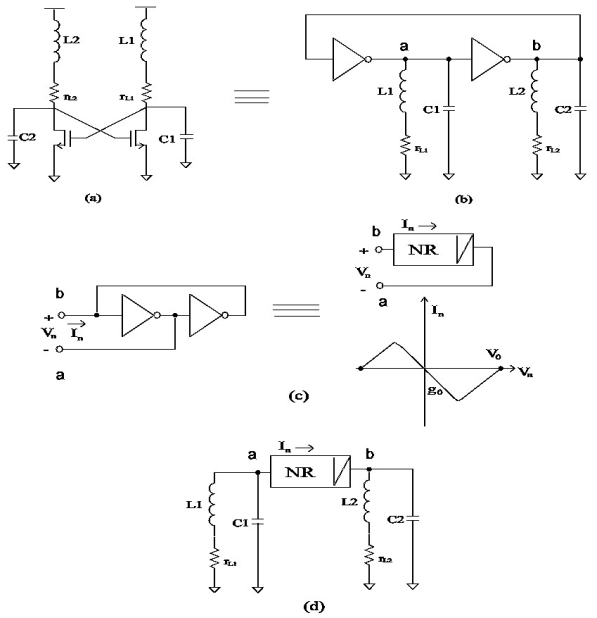

Figure 1: (a) Cross-coupled oscillator and (b) its inverter-based equivalent. (c) Voltage-controlled nonlinear resistor formed of two inverters and (d) 4-D oscillator model.

II. Proposed 4D nonlinear model

It is known that two invertering amplifiers connected as shown in Fig. 1(c) form a monotone voltage-controlled cubic-type differential negative resistor whose characteristics can be modelled by [9], [10]

$$I_n = g_0 V_n [(\frac{V_n}{V_0})^2 - 1] \qquad (1)$$

I_n is the current flowing into the resistor, V_n is the voltage across the resistor, V_0 is the zero crossing voltage (see Fig. 1(c)) and g_0 is the slope at the origin in Amp/V. It is clear that around the origin ($V_n << V_0$), the differential resistance is negative and equal to $1/g_0$.

With reference to Figs. 1(b) and 1(c) and noting the location of the two nodes labelled a and b respectively, it is possible to model the oscillator of Fig. 1(a) as shown in Fig. 1(d). Note that resistors $r_{L_{1,2}}$ represent both the inductors' internal parasitics and the inverters' resistive loads. Also note that it is always possible to transform any series reactance X_s and resistance R_s into a parallel susceptance X_p and resistance

R_p using the simple transformation $R_p = (R_s^2 + X_s^2)/R_s$ and $X_p = -X_s/(R_s^2 + X_s^2)$. Hence, a parallel tank resonator and a series resonator are essentially equivalent.

Figure 1(d) is described by the following equations

$$L_1\dot{I}_{L_1} = V_{C_1} - r_{L_1}I_{L_1}\ ,\ L_2\dot{I}_{L2} = V_{C_2} - r_{L_2}I_{L_2} \quad (2a)$$

$$C_1\dot{V}_{C_1} = I_n - I_{L_1}\ ,\ C_2\dot{V}_{C_2} = -I_n - I_{L_2} \quad (2b)$$

where I_n is as given by (1) with $V_n = V_{C_2} - V_{C_1}$. Common practice usually implies identical resonators; i.e. $C_1 = C_2 = C$, $L_1 = L_2 = L$ and $r_{L_1} = r_{L_2} = r_L$.

Introducing the dimensionless variables: $x(t) = V_{C_1}(t)/V_0$, $y(t) = V_{C_2}(t)/V_0$, $z(t) = r_{L_1}I_{L_1}(t)/V_0$, $w(t) = r_{L_2}I_{L2}(t)/V_0$, $q = \sqrt{L/C}/r_L$, $A_d = g_0 r_L$ and normalizing time with respect to $\sqrt{LC}$, the above circuit equations transform into

$$\begin{pmatrix} \dot{x} \\ \dot{y} \\ \dot{z} \\ \dot{w} \end{pmatrix} = \begin{pmatrix} -A_n \cdot q & A_n \cdot q & -q & 0 \\ A_n \cdot q & -A_n \cdot q & 0 & -q \\ 1/q & 0 & -1/q & 0 \\ 0 & 1/q & 0 & -1/q \end{pmatrix} \begin{pmatrix} x \\ y \\ z \\ w \end{pmatrix} \quad (3a)$$

$$A_n = f(y,x) = A_d[(y-x)^2 - 1] \quad (3b)$$

Note that q in the above model is the quality factor of the tank circuit while A_d is a differential gain since g_0 is related to g_m as $g_0 = g_m/2$ and $g_m r_L$ is the gain of each common-source amplifier (inverter).

At the origin where $(y-x)^2 << 1$ the nonlinear gain $A_n \approx -A_d$ and the four eigenvalues of the system at this point are found to be

$$\frac{1}{2q}(-1 \pm j\sqrt{4q^2 - 1}) \quad \text{and} \quad (4a)$$

$$\frac{1}{2q}(2q^2A_d - 1 \pm j\sqrt{4q^2 - 4q^2A_d - 4q^4A_d^2 - 1}) \quad (4b)$$

The first eigenpair given by (4a) can give rise to sinusoidal oscillation with a normalized frequency[1] $\omega_n = 1$ only if $q \to \infty$; i.e. with a lossless tank. However, since q is finite, this eigenpair is always located in the left-half plane and cannot provide sustained oscillations. It remains to investigate the second eigenpair of (4b). Recalling the widely spread oscillation condition $g_m r_L \geq 1$, which is equivalent to $A_d \geq 1/2$ [8], and consulting (4b) exactly at $A_d = 1/2$ reveals that this eigenpair is then located at $\frac{1}{2q}(q^2 - 1 \pm j\sqrt{2q^2 - q^4 - 1})$. It is seen that for any $q > 1$, this complex pair splits into two real eigenvalues; one of which is always positive. Hence, the resulting oscillations are not sinusoidal but are rather relaxation-type oscillations [4]. As $x(t)$ and $y(t)$ increase, the term $(y-x)^2$ dominates resulting in A_n becoming positive and the system turning into a stable dissipative system. This mechanism maintains bounded relaxation oscillations. The maximum amplitude of oscillation can be approximated by equating $A_n = 0 \to (y-x)^2 = 1$. If the two inverters in Fig. 1(b) operate within their bandwidth and introduce no extra nonideal phase-shift then $x = -y$ and hence $x_{\max} = y_{\max} = 1/2$ [2].

[1]The de-normalized frequency $\omega_0 = \omega_n/\sqrt{LC} = 1/\sqrt{LC}$ since time is normalized with respect to $\sqrt{LC}$.

[2]This means $V_{C_1\max} = V_{C_2\max} = V_0/2$.

Figure 2 shows the waveforms obtained from numerical integration of (3) at $A_d = 1/2$ with $q = 5$. The cubic nonlinearty, plotted dynamically during oscillations, is also shown in the figure. The waveforms are typical for relaxation oscillators and indeed $x_{\max} = y_{\max} \approx 1/2$.

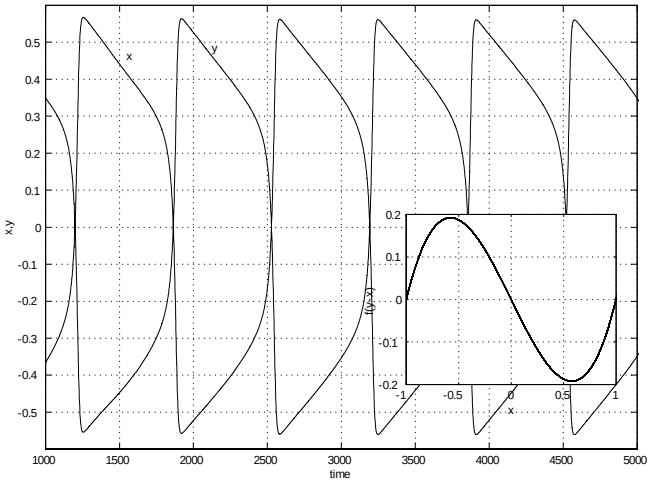

Figure 2: Relxation oscillations obtained from the 4D model of the cross-coupled oscillator with $A = 1/2$ and $q = 5$. Cubic nonlineaity is shown in the subplot.

Consulting (4b) again, it is seen that the correct condition for oscillation is

$$A_d \geqslant \frac{1}{2q^2} \to g_m \geqslant \frac{r_L}{L/C} \quad (5)$$

which places the eigenpair of (4b) on the $j\omega$ axis. To start oscillations, the eigenpair should be slightly shifted into the right-half plane implying $A_d > 1/2q^2$. The frequency of oscillation is then given by

$$\omega_n = \sqrt{1 - 1/q^2} \quad (6)$$

which simplifies to $\omega_n = 1$ ($\omega_0 = 1/\sqrt{LC}$) for $q >> 1$. It can also be shown that for a fixed gain A_d, the maximum amplitudes $x_{\max} = y_{\max} \leq \sqrt{1 - \frac{1}{2q^2A_d}}$. Figure 3 shows the waveforms obtained from numerical integration of (3) at $A_d = 0.025$ with $q = 5$ along with the dynamically plotted cubic nonlinearity. Note from (5) that the oscillation condition in this case is $A_d \geq (1/50 = 0.02)$.

It should be noted that the condition for oscillation (5) applies only at the origin ($x(t) = y(t) = 0$) whereas the real-time condition depends on the amplitudes of $x(t)$ and $y(t)$ and is given by

$$A_d \geq \frac{1}{2q^2[1 - (y-x)^2]} \approx \frac{1}{2q^2(1 - 4x^2)} \quad (7)$$

This condition implies that for a fixed A_d and as the oscillation amplitude grows, a point at which the oscillation condition will not be satisfied (hence oscillations seize) is guaranteed. Alternatively, in order to oscillate, the two inverters of Fig. 1(b) should be designed such that their input-output ($V_i - V_o$) characteristics satisfy the relation

$$A_d = \frac{|V_o|}{|V_i|} \geqslant \frac{1}{q^2(1 - 4(\frac{V_i}{V_0})^2)} \quad (8)$$

Figure 4 is a plot of this boundary curve at $q = 5$ and at $q = 1$ respectively indicating the regions where oscillations are possible. It is clear that the lower the quality factor, the sharper the needed amplifier characteristics (i.e. higher gain is needed). Note in Fig. 4 that normalized input $(V_{ni} = V_i/V_0)$ and output $(V_{no} = V_o/V_0)$ are plotted. For comparison, we have also plotted the nearest two approximate curves given by the hyperbolic tangent nonlinearities $V_{no} = -\tanh(V_{ni}/20)$ and $V_{no} = -\tanh(V_{ni})$ respectively.

Equation (8) thus describes a simple graphical design method whereby it is required to optimize the $V_i - V_o$ nonlinear transfer curve for each inverter to be as close as possible to the boundary curve at a given q, as demonstrated in the following section.

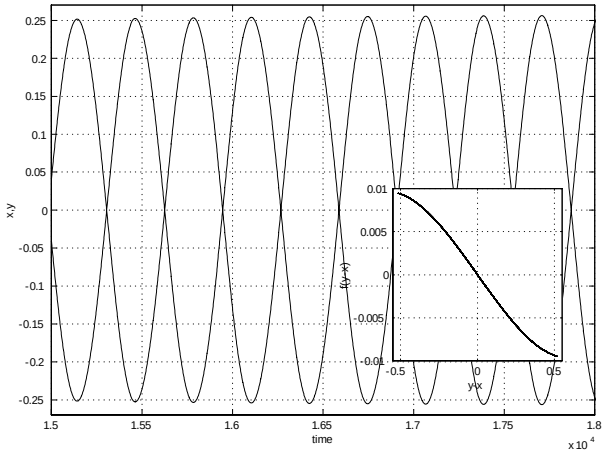

Figure 3: Sinusoidal oscillations obtained from the 4D model of the cross-coupled oscillator with $A_d = 0.025$ and $q = 5$. Cubic nonlineaity excursion is shown in the subplot.

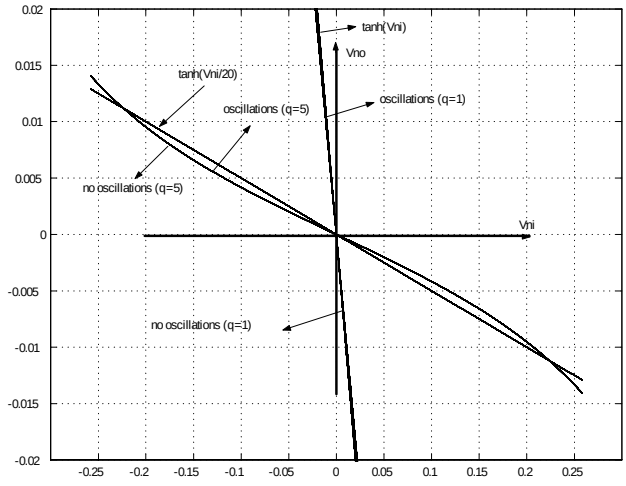

Figure 4: Boundary transfer characteristics for the two inverters to oscillate at $q = 5$ and $q = 1$ respectively.

III. Design Example

The oscillator in Fig. 1(a) was designed to oscillate at 20Mhz with $L = 1\mu H$, $C = 64pF$ and $r_L = 25\Omega$, which sets $q = 5$. Hence, the condition to start oscillation is $A_d = 25g_0 > (\frac{1}{2q^2} = 0.02)$; i.e. $g_0 > 0.8mA/V$. The design process requires choosing the MOS transistors' aspect ratios (W/L) as well as suitable biasing positive and negative supply voltages (V_{cc} & V_{ss} respectively) in order to ensure sustained oscillations with g_0 as close as can be to its theoretical value $(0.8mA/V)$. The graphical nonlinear design process can be followed where it is required that while oscillations are sustained:

(i) the cubic nonlinearity curve be as close as possible to the cubic nonlinear curve plotted in Fig. 3 for $q = 5$

(ii) the transfer characteristic for each inverter be as close as possible to the ideal boundary curve plotted in Fig. 4 at $q = 5$.

Figure 5 shows Spice simulation results obtained with $W/L = 11\mu/1\mu$, $V_{cc} = +0.25V$ and $V_{ss} = -1.75V$ using a 0.25μ CMOS process parameters. The cubic nonlinearity $[(I_{C1} - I_{C2} + I_{L2} - I_{L1})$ versus $(V_{C1} - V_{C2})]$, dynamically plotted during simulations, is shown in the middle trace of Fig. 5 from which g_0 is measured to be $1.4mA/V$ and hence $A_d = 0.036 > 0.02$. Below this value, oscillations cannot start. Using (7) with this value of A_d, the amplitude $x_{\max}$ is found to be 0.33 and hence $V_{C_{1,2}\max} = 0.33V_0 \approx 1V$ $(V_0 \approx 3V)$. The lower trace shows the inverter input-output transfer characteristic (V_{C1} versus V_{C2}) in this case compared to the ideal oscillation boundary which from Fig. 4 at $q = 5$ can be approximated by $V_{no} = -\tanh(V_{ni}/20)$. Note that the nonlinear graphical design process does not require any knowledge of the specific MOS transistor technology parameters[3] and that this process can be automated via a batch simulation file in search for optimum V_{cc}, V_{ss} and/or W/L.

Close inspection of the nonlinearity in the middle trace of Fig. 5 reveals a very weak hysteresis effect. In particular, as A_d is increased much, a hysteresis loop becomes apparent, as shown in Fig. 6 for $W/L = 50\mu/1\mu$. This will give rise to relaxation rather than sinusoidal oscillations which is what happens when using the widely spread condition $A_d > 1/2$, implied by the Barkhausen criterion.

Finally, it is important to note here that in driving the nonlinear 4-D model (3) we have assumed the two inverters to be frequency independent; i.e. we have not considered the internal MOS parasitic capacitors unless they appear in parallel with C_1 or C_2. Thus the 4D model remains valid only within the bandwidth of each common-source amplifier (inverter).

IV. Conclusion

We have proposed a 4D nonlinear model for cross-coupled oscillators and a more accurate condition for oscillation. A nonlinear graphical design optimization procedure was explained.

References

[1] A. Borys, "Elementary deterministic theories of frequency and amplitude stability in feedback oscillators," IEEE Trans. Circuits & Syst.-I, vol. 34, pp. 254-258, 1987.

[2] A. S. Elwakil, and W. Ahmed, "On the necessary and sufficient conditions for latch-up in sinusoidal oscillators," Int. J. Electronics, vol. 89, pp. 197-206, 2002.

[3] M. P. Kennedy and L.O. Chua, "Hysteresis in electronic circuits: A circuit theorist's perspective," Int. J. Circuit Theory & Applications, vol. 19, pp. 471-515, 1991.

[3]Recall that $g_0 = g_m/2 = \sqrt{2\mu_n C_{ox}\frac{W}{L}I_{DS}}/2$. μ_n is the electron mobility, C_{ox} is the oxide capacitance, W is the transistor width, L is the transistor length and I_{DS} is the DC biasing current.

[4] A. S. Elwakil, “Low voltage relaxation oscillator,” Electronics Letters, vol. 36, pp. 1256-1257, 2000.

[5] A. Hajimiri and T. Lee, “Design issues in CMOS differential LC oscillators,” IEEE J. Solid-State Circuits, vol. 34, pp. 717-724, 1999.

[6] Z. Li and K. Kenneth, “A low-phase-noise and low-power multiband CMOS voltage-controlled oscillator,” IEEE J. Solid-State Circuits, vol 40, pp. 1296-1302, 2005.

[7] F. Yuan, “A fully differential VCO cell with active inductors for Gbps serial links,” Analog Integrated Circuits and Signal Processing, vol. 47, pp. 213-223, 2006.

[8] B. Razavi, “A Study of Phase Noise in CMOS Oscillators,” IEEE Journal of Solid-State Circuits, vol. 31, pp. 331-343, 1996.

[9] L. O. Chua, C. Desoer, and E. Kuh Linear and nonlinear circuits, McGraw-Hill, 1987.

[10] K. O’Donoghue, M. P. Kennedy and P. Forbes, “A fast and simple implementation of Chua’s oscillator using a "cubic-like" Chua diode,” Proc. European Conf. on Circuits Theory & Design ECCTD’05, vol. II, pp. 83-86, Cork, Ireland, 2005.

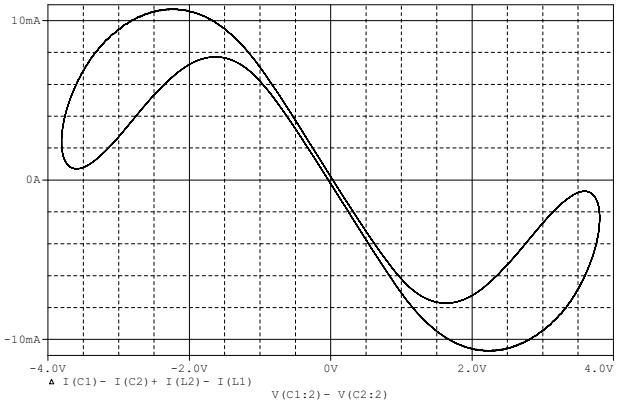

Figure 6: Hysteresis effect in the cubic nonlinearity as A_d is increased $(W/L = 50\mu/1\mu)$.

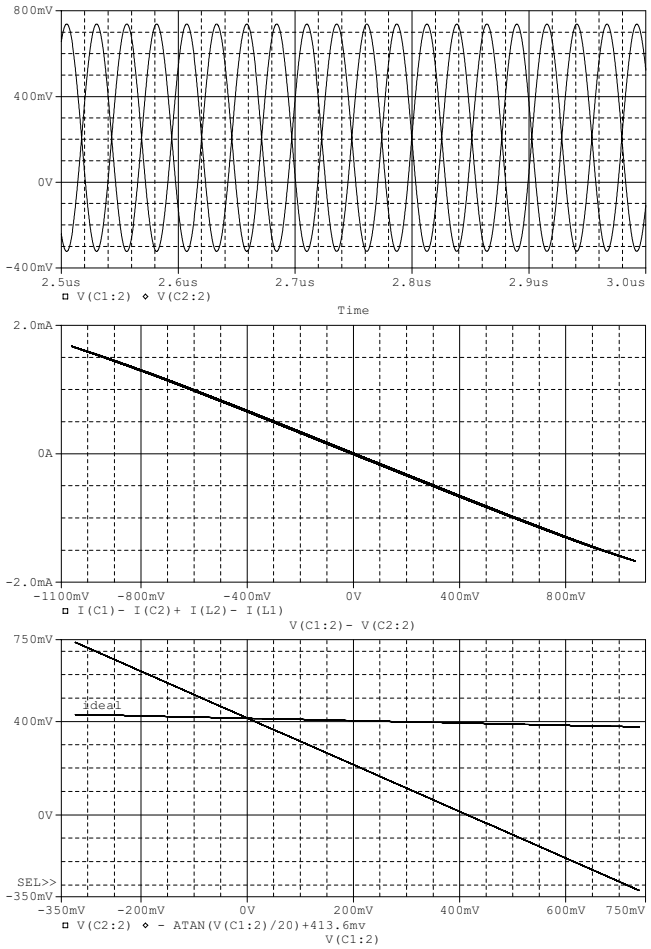

Figure 5: Spice simulations with $L = 1\mu H$, $C = 64pF$, $r_L = 25\Omega$, $W/L = 11\mu/1\mu$, $V_{cc} = +0.25V$ and $V_{ss} = -1.75V$. Upper trace: V_{C1} and V_{C2} time waveforms. Middle trace: dynamically plotted cubic nonlineaity. Lower trace: $V_{C1}-V_{C2}$ inverter transfer characteristic versus ideal oscillation boundary at $q = 5$.